Elephants have an adaptable prehensile grip

Andrew K. Schulz[1,2], Joy S. Reidenberg[3], Jia Ning Wu[1], Cheuk Ying Tang[4], Benjamin Seleb[5], Josh Mancebo[6], Nathan Elgart[6], and David L. Hu[1,5*]
Schools of Mechanical Engineering[1] and Biological Sciences[5]
Georgia Institute of Technology, Atlanta, GA 30332, USA
Max Planck Institute for Intelligent Systems[2], Stuttgart, Germany
Center for Anatomy and Functional Morphology[3]
Radiology, Neuroscience, & Psychiatry Translation and Molecular Imaging Institute[4]
Icahn School of Medicine at Mount Sinai, New York, NY
Zoo Atlanta[6], Atlanta, GA 30315, USA

October 6, 2022

Corresponding author:
David L. Hu
801 Ferst Drive, MRDC 1308, Atlanta, GA 30332-0405
(404)894-0573
hu@me.gatech.edu

Keywords:
weight lifting, power, capstan

Abstract

Although it is well-known that elephants use their trunk in a prehensile fashion, little is known about the mechanics of their grip. In this study, we show that an African elephant recruits greater length of its trunk with increasing weight lifted. We measure the wrinkle and trunk geometry from a frozen elephant trunk at the Smithsonian and challenge a female African elephant at Zoo Atlanta to lift various barbell weights using only its trunk. The elephant lifts a 60-kg weight at a speed of 1 m/s, employing 450 watts of power. Increasing weights cause the trunk's contact area with the weight to increases six-fold. Our findings may inspire the design of more adaptable soft robotic grippers.

1 Introduction

Prehension is the ability to grasp or seize by wrapping around (Jones-Engel & Bard, 1996). Many tree-foraging animals evolved prehensile appendages to grasp branches (Garber & Rehg, 1999; Hickman, 1979; Hoffmann, Montag, & Dominy, 2004; Negrea, Botnariuc, & Dumont, 1999). While this behavior has long been observed, there have been few systematic studies of the mechanics of prehensile gripping. In the following study, we train elephants to lift weights with their trunk.

Prehensile tails are thought to have evolved in the dense South American forests, where animals often traverse narrow supports and distribute their weight to the surrounding canopy (Emmons & Gentry, 1983; McGinn, 2015). The most well-known examples of prehensile animals are the Atelinae, a subfamily of monkeys that includes howler and spider monkeys (Laska, 1998). Both spider and howler monkeys can hang their entire body weight (up to 10 kg) from their tail, a behavior that frees their hands to manipulate fruit (Laska, 1996). Such strength requires substantial musculature, innervation to control the tail, and a particular region in their brain for tail control.

Another adaptation that makes these monkeys more prehensile than their relatives the capuchins, is their friction pad, a hairless and highly sensitive strip of skin on their tail (Organ, Muchlinski, & Deane, 2011). Capuchins in contrast have a tail that is covered in fur. Due the monkey's quick movement through the dense canopy, there is little measurement of how they grip branches with their tail (Russo & Young, 2011). In this study, we hope to improve our understanding of prehensile appendage use in systematic experiments with highly trainable African elephants.

While Atelines can support their entire body using their tail, six lineages of mammals evolved prehensile but weaker tails. The tamandua, an arboreal anteater uses its tail for support while feeding (Cartmill, 1972). Giraffes have a prehensile tongue used to grasp leaves and clean their faces (Pretorius et al., 2016). Seahorses don't swim with their tail; instead they use it anchor onto coral. A unique aspect of the seahorse tail is its square-shaped cross section, which increases contact area with the substrate (Lourie, Pollom, & Foster, 2016). Moreover, when compressed in the jaws of a predator, the square tail better survives compression than a circular tail (Porter, Adriaens, Hatton, Meyers, & McKittrick, 2015).

Many tools in the human-built world such as knobs, steering wheels, and door handles, were designed to be operated by the human hand. Thus, there has been much interest in robotics in building prehensile manipulators (Iberall, 1997). The human hand has five fingers, over 25 degrees of freedom, and three grasping motor primitives (transverse, perpendicular, or parallel to the palm). Motor primitives are described as neural mechanisms that assists with coordinated motions. Different postures present varying degrees of force, motion, and sensory information (Iberall, 1997). Like the human hand, the elephant can move with both precision and and high force. While the 3D kinematics of the elephant trunk grasping different shaped objects has been recently recorded, the weight of these objects was not varied (Dagenais, Hensman, Haechler, & Milinkovitch, 2021; Schulz et al., 2021; Wu et al., 2018). In this study, we consider how object weight affects the elephant's prehensile grip. Our observations of the degree of wrapping may inspire more quantitative studies of prehensile behavior and the design of prehensile robotics.

We begin in §2 with our experimental methods for working with elephants. In §3, we present our calculations of trunk tension, power, and surface area. We report the results of our experiments in §4. We then discuss the repercussions of our work in §5 and conclude in §6.

2 Materials and Methods

2.1 Elephant experiments

Experiments were performed with a 35-year-old female African Elephant (*Loxodonta africana*) of mass 3360 kg and height 2.6 m. We conducted experiments outdoors, at the edge of the elephant's enclosure at Zoo Atlanta. The experiments occurred over two-hour periods in the mornings of spring and summer 2018 before Zoo Atlanta opened to the public. The staff at Zoo Atlanta supervised all experiments.

To train the elephant to lift, the zookeepers used a reward system beginning with gesturing the elephant towards the barbell (**Figure 1**b). If the elephant accomplished the correct task of grabbing and lifting the bar, food was rewarded(**Figure 1**c-d). If an incorrect outcome was observed, then the experimental procedure was repeated until the trial was successful. Once an 80% success rate was achieved, we commenced weightlifting experiments (**Figure 2**a). It took 15 attempts and 10 minutes of training to accomplish an 80% success rate.

Experiments were conducted with a Smith Machine (Powerline PSM144X, 2.0 x 1.1 x 1.9 m), which uses twin friction-less carriages to constrain the barbell to move vertically. The barbell was placed at a set distance of $w = 0.5 \pm 0.05$ m (n=22) away from the enclosure bars. As a result of this distance, the elephant had to rely on its trunk to lift. Without the restraint of the bars, the elephant would likely use a combination of its forehead, trunk, and tusks to lift heavy objects.

Iron weight plates were added to the 20-kg bar to provide the elephant a set of six weights comprising 20, 25, 30, 35, 43, and 60 kg. The elephant completed four trials of each weight with a food reward and one minute rest between each lift. When weights were changed, five minutes of rest was given to change the weights and re-secure the frame to the ground using 80 kg of barbell weights.

Twenty-two barbell lifts were filmed using a high-definition digital video camera (Sony HDRXR200) and iPhone 8. We tracked the position of the weight along the 2.0 m height of the Smith machine to accurately determine the barbell height. In two trials, the elephant barely lifted the bar above its original position; such experiments were considered incomplete, and the data was not analyzed. Analysis of the elephant lifting 50 kg was removed from the analysis because the elephant broke the Smith machine during the 50 kg test. During testing the elephant struggled to lift the 60 kg barbell and only proceeded to lift it twice. We tracked the trunk by first drawing along a line of chalk on the mid-line of the right lateral side of the elephant trunk. Using Tracker, an open-source video analysis tool (https://physlets.org/tracker/), we tracked 60 equally spaced points along this line. The speed and acceleration of the elephant lift were determined by tracking the barbell side-view position.

2.2 Dissection of an elephant trunk

Icahn School of Medicine at Mount Sinai, New York provided access to a frozen trunk from a 38-year old female African elephant, *Loxodonta africana*, that initially lived in a Virginia zoo. Detailed information about the elephant can be found in the pathology report (**Supplemental Figure 1**). The elephant's body weight before death was approximately 4000 kg, and the weight, age, and sex of this elephant are comparable to those of the elephant filmed in our study. The trunk was cut into several parts and stored in a freezer in 2015 at $-15°C$ until we dissected it in July of 2016. In January of 2018, the specimen's distal tip was fully thawed and scanned on a Siemens Dual Source Force CT to measure the trunk's nasal passageways and outer diameter at an acquisition speed of 737 mm/sec and a temporal resolution of 66 msec (**Figure 3**a-b, **Supplemental Video 4**). A helical scan was performed with 80 kV, 183 mAs, and a slice thickness of 0.5mm. We scanned the distal portion of the trunk up to around 110 cm from the tip as more of the trunk would not fit in the CT scanner. We obtained 27 measurements of the trunk's diameter inner diameter as the scan progressed from proximal root to distal tip (**Figure 4**c). We also rendered the entire CT image of the trunk to see the three-dimensional structure (**Supplemental Video 5**).

3 Mathematical Modeling

3.1 Elephant trunk geometry

We modeled both the elephant trunk and its nasal cavities as conical frustums (Read, 1937). Assuming the mass density of the trunk is $\rho = 1180$ kg/m^3, measured from a cross-section of an elephant carcass' trunk (Wilson, Mahajan, Wainwright, & Croner, 1991), the mass m_t of a trunk segment of length z may be modeled using a frustum exterior with two frustums as nasal cavities. With these assumptions, the mass may be written (Bland, 1954):

$$m_t(z) = \frac{\pi \rho z}{3}\left[R^2(z) + R(z)R(0) + R^2(0) - 2\left(r^2(z) + r(z)r(0) + r^2(0)\right)\right]. \quad (1)$$

The length z is measured from the trunk tip, and $R(z)$ and $r(z)$ are, respectively, the outer and inner radii of the trunk at a position z. Based on the frozen trunk measurements, the radii for the trunk tip are $r(0) = 1.1$ cm and $R(0) = 2.2$ cm. The nasal passages of the frozen trunk were squashed by self-weight; thus, we used the nasal circumference to extrapolate the inner radius (**Figure 4**d).

3.2 Tension and power applied

To determine the force required to lift the barbell, we considered a vertical force balance on the trunk tip. A control volume is shown schematically in **Figure 5**a. When the barbell is lifted, the elephant lifts both the barbell and the trunk itself. The total mass to be lifted is $m = m_t + m_b$ where m_b is the barbell mass and m_t is the mass of the trunk segment in contact with the barbell. The height of the trunk segments not in contact cannot be calculated without image analysis. Thus, a weakness of our method is that force and power will be under-estimated.

The angle ϕ to the horizontal is measured when the trunk first begins lifting the barbell (**Figure 5**a). The trunk exerts a tension T to lift. We neglect the displacement in the horizontal direction because the Smith Machine constrains the lift to the vertical direction. Since the trunk segment is wrapped around the barbell, both move with the same vertical speed $\dot{y}$ and acceleration $\ddot{y}$. By Newton's law, the vertical force balance may be written

$$m\ddot{y} = -mg + T \sin\phi, \tag{2}$$

where g is the acceleration of gravity and T is the tension applied. Solving Equation (2) with respect to the tension force T yields

$$T = \frac{m(\ddot{y} + g)}{\sin\phi}. \tag{3}$$

Thus, by measuring the angle ϕ and the acceleration $\ddot{y}$, we can estimate the force exerted to lift the barbell.

We calculate the power to lift two parts of the trunk, the tip and the base, which is located 160 cm from the tip. Each of these parts has its own mass that is estimated from Equation (1). The average power exerted to lift part i of the trunk may be written as the ratio of the gravitational potential energy and duration t of lift. The gravitational potential energy of a trunk segment of mass m_i is written as $U = m_i g y_i$, where y_i is the change in the height of the center of mass of that portion of the trunk. The power is thus

$$P_i = \frac{m_i g y_i}{t}, \tag{4}$$

which is consistent with the definition of power for human weight lifters (Jones, Fry, Weiss, Kinzey, & Moore, 2008).

3.3 Contact area

The ventral part of the trunk is flat but covered with wrinkles. To estimate the contact area of the trunk and the barbell, we measure the frequency ω and amplitude A of the trunk wrinkles at eight positions along the frozen elephant trunk with 10 different azimuthal positional measurement around the ventral section taken at each position. Previous measurements of strain during extension shows that the tip of the trunk, defined as the last 30 cm, stretches less than 10% strain, which is small compared to stretch mid-distally, which is 25 percent(Schulz et al., 2022). We thus assume that the wrinkle geometry of the un-extended frozen trunk matches the live elephant. Assuming a sinusoidal wrinkle profile, the radius R of the ventral trunk skin as a function of distance z from the tip is written in the results section in Equation (4.3).

We report the amplitude $A(z)$ and frequency $\omega(z)$ in the results section and in **Figure 7**E-F. To calculate the surface area of contact of a trunk segment, we utilize the arclength formula which states the arclength s of the trunk segment is

$$s = \int_{z=z_0}^{z=z_f} \sqrt{1 + (\frac{dR}{dz})^2}. \tag{5}$$

This integral is calculated numerically using MATLAB ode45, between the two points z_0 and z_f, which defines the trunk segment in contact with the bar. We assume the contact region is a wrinkled planar trapezoid of height s, and lengths $D(z_f)$ and $D(z_0)$, which are the diameters of the trunk at the points z_f and z_0. The area of this trapezoid is :

$$SA = s \cdot \frac{D(z_f) + D(z_0)}{2}, \tag{6}$$

where we have assumed that the peaks and troughs and all the surface area of the wrinkles contact the bar.

4 Results

4.1 Trunk geometry

To calculate the force applied by the trunk, we first measure its shape. We characterize frozen trunk from the Smithsonian using CT-scanning and dissection (**Figure 3**, **Supplemental Video 4**). At the proximal base, the cross-section is dominated by radial muscle shown by the light-colored muscle close to the nasal cavities. The large amount of radial muscle is presumably to help with lifting as the base does not stretch much longitudinally (**Figure 4**e) (Schulz et al., 2022). The longitudinal muscle is darker red and lies between the radial muscle and the skin of the trunk. The proportion of radial muscle shrinks progressively towards the distal tip, while the proportion occupied by the nostrils increases. The distal tip of the trunk lacks radial muscle and is instead dominated by two oblique muscle groups (**Figure 4**b), which assist with wrapping around objects, such as the barbell, as they come into contact.

The trunk is a hollow conical frustum permeated by a pair of nostrils. From the CT scans, we obtain a relationship for both the inner and outer radius of the trunk at a distance from the tip, z (**Figure 4**a). The inner radius r is given by the open triangles and outer radius R by the closed points. The solid lines are linear least squares best fits given by

$$r(z) = 0.011 + 0.0002z, (R^2 = 0.95), \tag{7}$$
$$R(z) = 0.022 + 0.0006z, (R^2 = 0.99), \tag{8}$$

with all units in meters. At the tip, the inner and outer radii are 1.1 cm and 2.2 cm. At a point 100 cm from the tip, the trunk has an inner and outer radii of 3 cm and 8 cm. By integrating the volume of the trunk, Equation (1), we find that the trunk mass is 97 kg, which is close to the experimental measurement of 110 kg. The mass m_t of the trunk segment in contact with the barbell was calculated for each experiment based on the length in contact. The weight of the trunk in contact ranged from 5.4 kg for the lightest barbell up to 9.0 kg for the heaviest.

4.2 Lifting force

The elephant lifts the barbell by first wrapping its trunk tightly around it (**Figure 1**). Although the trunk is initially straightwhen it reaches for the barbell, the trunk arches as it lifts (**Figure 2**a and **Supplemental Video 1-3**), acting like a bending beam supporting a load at its tip. The total energy expended for each barbell weight is related to the maximum height of the lift y_{max}, shown in **Figure 2**c. The linear best fit, shown by the dashed line, is

$$y_{max} = 1.64 - 0.026m_b, (R^2 = 0.95) \tag{9}$$

where y_{max} is the height lifted in meters. For this and future equations, m_b is the weight of the barbell in kg. The elephant lifted the lightest weight to a height of 1.19 ± 0.1 m (n=4) , nearly touching the top of the weight rack, and the heaviest weight to less than one-tenth the height 0.1 ± 0.05 m (n=2). Clearly, the elephant lifted heavier weights to lower heights. The x-intercept of Equation (9) shows that that the maximum weight that elephants can lift in this setup is 63 kg, which is just 2% of its body weight and 65% of its trunk weight. We surmise that the barbell apparatus constrains the elephant's trunk motion to the vertical direction, which prevents the elephant from using body weight to push or lift the object.

The time course of the barbell height y_b is shown in **Figure 2**b, where we spaced out the trajectories for clarity. After the trunk wrapped around the barbell, the lifts were fast, taking approximately $0.5 - 0.8$ s across the weight classes. Each function was fit with two quadratic best fits separated by an inflection point between the acceleration and deceleration phases. The inflection point usually occurs midway of the lift duration. In the acceleration phase, the position may be written as $y_b = at^2$ where t is time and a is the acceleration. This equation describes lifting from a rest position with a constant acceleration a. Such a relationship fits the acceleration phase well, with an R^2 greater than 0.95. The deceleration phase was fit with the position and velocity at the inflection point, as well as a constant deceleration: $y_b = y_0 + vt - bt^2$. We found no clear trend between deceleration and barbell mass, so the deceleration was not reported. The fits for the entire lift are shown in **Figure 2**b. The acceleration $\ddot{y}_b = a$ for each barbell mass is shown in **Figure 2**d, with the linear best fit given by

$$\ddot{y}_b = 4.49 - 0.043m_b, (R^2 = 0.63), \tag{10}$$

where $\ddot{y}_b$ is in m/s^2 and m_b is in kg. Equation (10) indicates that an elephant has a lower acceleration for heavier weights: acceleration ranges from 3.9 m/s^2 for the lowest weight to less than half that value for a weight three times heavier.

Upstream of the trunk, lifting the barbell is accomplished by some combination of rotation and lifting of the head. We measured the position of the trunk base, defined as the trunk region 160 cm from the tip. We located this point in the video by the apex of the tusk. The blue points in **Figure 2**d shows the vertical acceleration of the trunk base: the acceleration of 1 m/s^2 is small compared to most of the trunk tip accelerations. We conclude that the neck is not lifting. Instead, it acts like a fulcrum to provide rotational motion to assist lifting by the trunk tip.

To calculate the tension applied by the trunk, we measured the angle that the trunk intersects the barbell. **Figure 5**b gives the angle ϕ of the trunk with respect to the horizontal, where the dashed line is the least square linear best fit. The relationship between angle of trunk and barbell mass is

$$\phi = -6.4 + 1.6m_b, (R^2 = 0.94), \tag{11}$$

with ϕ in degrees. An angle of 90 degrees indicates that the elephant orients its trunk vertically.

The elephant increases the angle of contact ϕ from $23 \pm 3°$ (n=4) for the lightest weight to nearly four times that amount, or $89 \pm 2°$ (n=2), for the heaviest.

Given the angle of contact, ϕ, and the length of the trunk z wrapped around the bar, we calculate the trunk tension T using Equation (3) in the Math Methods. The relationship between tension and the mass lifted is shown in **Figure 5**c. Although the barbell weights increase by a factor of three, the tension increases by only 20%, maintaining an average value across all trials of 620 ± 64 N (n=22). We thus see that elephants have dual "strategies" to reduce tension when lifting heavy weights: they decrease acceleration and orient their trunk more vertically. These strategies may not be volitional: they may simply arise from trying to lift a heavier weight with a finite muscle of limited force and power. Nevertheless, we see the trunk adapts to different postures and kinematics for different weights.

Figure 6b shows the relationship between power exerted and the mass lifted, with red points referring to the trunk base and black points to the trunk tip. These powers are over-estimates because they only consider the maximum deflection of the highest point rather than the center of mass of each section. The power-expenditure of the tip is U-shaped, with a peak power of 357 ± 79 W (n=4) for intermediate masses. No matter what weight lifted, the power expended at the trunk base remains higher than the trunk tip.

4.3 Prehension

Although the elephant was a constant distance to the bar, it wrapped a greater length of its trunk to lift heavier weights. **Figure 6**a shows the progression of trunk wrapping, from $\theta = 87 \pm 6°$ (n=4) to $400 \pm 12°$(n=2), an increase of 400% in wrapping angle. In order to lift the lightest weights (m_b = 20 and 25 kg), the trunk's distal tip extended past the barbell and wrapped around the bottom half, creating a lip that kept the barbell in place. When lifting medium weights ($m_b = 30 - 43$ kg), the trunk extended further, using a thicker section of its trunk to wrap. And finally when the elephant lifted the heaviest weight ($m_b = 60$ kg), the trunk wrapped 413 degrees, or more than a full cycle.

Wrapping a greater angle increases the area of contact between the barbell and elephant trunk. We note that the largest angle that supports the weight of the barbell is 180 degrees, corresponding to the bottom half of the barbell. Any additional wrapping helps with stability rather than weight support.

For us to rationalize the increased wrapping angle with heavier weights, we consider the capstan, a rotating device that amplifies a sailor's ability to pull a rope (Gao, Wang, & Hao, 2015). The classical capstan model shows that $T_b/T_a = e^{-\mu\theta}$ where θ is the angle subtended by the capstan, μ is the coefficient of friction, and T_b/T_a is the ratio of the sailor's force to the force on the other end of the rope. Assisted by the friction on the rope wrapped around the capstan, the sailor can amplify its force T_b to support a load T_a.

Applying the capstan problem to the barbell wrapping, we may consider the "sailor" to be the gravitational force $T_b = m_t g$ imposed by the pendent mass m_t that is wrapped around the barbell.The weight of the pendent as well as the friction at the contact area opposes the barbell weight $T_a = m_b g$. By wrapping greater angles, the elephant can use the weight of the pendant to avoid losing grip on the barbell as it is lifted. Based on the arclength of trunk wrapped, the calculate the weight of the pendent mass varies from 5.4 to 9 kg, and increases with barbell mass. Simplifying the capstan model, we find

$$\theta = a \ln (b m_b) \tag{12}$$

where $a = \frac{1}{\mu}$ and $b = \frac{1}{m_t}$. A least-square best fit is given in red which fits the data quite well, showing that $100 - 300$ degrees of wrap is sufficient to hold the barbell (**Figure 6**a). The free parameter for the best fit is a high but physically reasonable friction coefficient of $\mu = 1.5$, comparable to the friction coefficient of 1.6 for bio-mimetic snake robots scales on styrofoam (Marvi, Meyers, Russell, & Hu, 2011). Snakes can change the angle of their ventral scales to increase frictional forces as they climb tree trunks and other vertical surfaces. Such actively deformable surfaces are analogous to the friction-enhancing wrinkles and coarse hair on the trunk. For comparison, we show in blue the another wrapping angle using the friction coefficient of human skin on metal ($\mu = 0.8$). Indeed, such a low friction coefficient requires wrapping angles of 200-500 degrees, which are higher than the observed angles. Both results bound the data and give rationale that the combination of self-weight of the pendant mass and friction of the skin prevent the barbell from slipping as it is lifted.

Our capstan model assumed a constant friction coefficient, but the trunk may be able to modify its friction coefficient using its wrinkled grip, as shown in **Figure 7**A. Assuming that the trunk surface has a sinusoidal wrinkle pattern, the wrinkle height may be written

$$y_{wrinkle} = A(z) \sin \frac{2\pi}{\lambda(z)} z \tag{13}$$

which is shown in **Figure 7**B. We measured by hand the amplitude A and wavelength λ as a function of the distance z from the tip. A linear least squares best fit shows that wrinkles increase both their amplitude and wavelength with distance from the tip:

$$A(z) = 0.0174z + 0.4461(R^2 = 0.95) \tag{14}$$

$$\lambda(z) = 0.036z + 0.051(R^2 = 0.97) \tag{15}$$

(**Figure 7**E-F) where A, λ, z are in cm. Using these relationships, we use equation Equation (6) to estimate the surface area of the wrinkled skin. As the barbell mass increases, the elephant wraps with increased arc length and greater surface area (**Figure 7**C). We consider two contributions to its surface area. First we consider a smooth ventral trunk devoid of wrinkles, shown by the black points (**Figure 7**D). The wrinkled surface area, from Equation (6) is shown in red. Since the tip has wrinkles of small wavelength, the additional surface area it provides is low. However, for the heaviest weight, the wrinkles contribute up to 15% of the surface area (**Figure 7**D).

5 Discussion

The Smith machine used in our experiments was designed for human weight lifting, but we were fortunate that the power generated by the elephant trunk is comparable to human power. When humans are lifting a barbell for a power clean, which involves lifting a barbell from the ground to the shoulders, they can achieve a power of 900 W on free weights, and 770 W on machine cleans for lifting just a 20 kg weight (Jones et al., 2008). When using just its trunk, the elephant lifts a 20 kg using only 238 ± 14 W of power, but could probably increase this amount with training.

To lift heavier weights, the elephant recruits greater surface area of contact using its trunk wrinkles. The ridges on human finger tips have been shown to increase friction by two mechanisms (Yum et al., 2020). On rough surfaces, the ridges deform and interlock into an uneven surface when gripping surfaces. This mechanism seems to also apply for elephants which often pick up rough objects such as tree bark, whose length scale of wrinkles seems a good match for the elephant wrinkles, whose wavelength varies from mm to cm. The other mechanism for human fingertips is more subtle, but involves the maintenance of an optimal layer of sweat between the ridges. The length scale of elephant wrinkles is much larger than human fingertip ridges; moreover elephants have very few sweat glands (Wright & Luck, 1984). Therefore it is unlikely that moisture plays a role in elephant grip.

In this study, we only examined the elephant lifting a barbell, but other works have shown that elephants also use their ventral trunk to lift a variety of size and shape of objects (Dagenais et al., 2021). While we only studied picking up a cylindrical barbell, gripping with the wrinkled surfaces may be important for picking up a range of objects. There remain many aspects to successful lifting that are not understood. In many prehensile animals, the surface of the skin is heavily innervated with sensors. The elephant's skin is substantially tougher than these animals; therefore it remains unknown how it can resist the elements of the African climate, yet still have a sensitive touch.

6 Conclusion

In this study, we elucidate the kinematic and gripping strategies elephants use to lift barbells. Elephants maintain nearly constant tensile force by orienting their trunk vertically and decreasing their acceleration for the heaviest weights. They increase their degree of wrapping with heavier weights, modifying their grip from a simple lip to prevent the bar from rolling out, to spiraling their trunk completely around the bar to increase stability. We showed that the self-weight of the trunk an be used like a sailor's capstan to prevent slipping of the barbell. Incorporating a greater length trunk also brings into play deeper and longer-amplitude wrinkles, which can engage with asperities in objects to increase friction. We hope that this work inspires new kinds of adaptable biologically-inspired grippers.

Conflict of Interest Statement

The authors declare no conflicts of interest in any of this manuscript.

Data Access Statement

We have included MATLAB files for the elephant lifts, raw elephant lifting trials, and data spreadsheets of strain tracking available for download on a GitHub repository that is linked in the supplemental documents.

Ethics Statement

In working with animals from Zoo Atlanta. We received research permits from both Zoo Atlanta and Georgia Institute of Technology.

Funding Statement

D.L.H., A.K.S., J.N.W. were supported by the US Army Research Laboratory and the US Army Research Office Mechanical Sciences Division, Complex Dynamics and Systems Program, under contract number W911NF-12-R-0011.

Acknowledgements

This work was supported by the US Army Research Laboratory and US Army Research Office Mechanical Sciences Division Complex Dynamics and Systems Program, under contact number W911NF-12-4-00111. We thank A. Lee, M. Chan, and Y. Zhang for their early contributions. We thank the Zoo Atlanta elephant keepers with their assistance in performing experiments. We thank Dr. Ali Nabaviziadeh for arranging the collaboration with Dr. Reidenberg. We thank the imaging time donated by Dr. Cheuk Tang's group, Radiology, Neuroscience, & Psychiatry Translation and Molecular Imaging Institute at Icahn School of Medicine at Mount Sinah. We thank J. Ososky and the Smithsonian Institution Museum of Natural History for their assistance with information regarding the frozen elephant trunk as well as loaning the elephant trunk to Icahn School of Medicine at Mount Sinah.

References

Bland, J. R. K. W. F. . (1954). *Solid Mensuration With Proofs Second 2nd Edition.* John Wiley & Sons.

Cartmill, M. (1972). *Arboreal Adaptations and the Origin of the Order Primates.* Routledge. Retrieved 2022-07-04, from `https://www.taylorfrancis.com/chapters/edit/10.4324/9781315132129-4/arboreal-adaptations-origin-order-primates-matt-cartmill` (Pages: 97-122 Publication Title: The Functional and Evolutionary Biology of Primates) doi: 10.4324/9781315132129-4

Dagenais, P., Hensman, S., Haechler, V., & Milinkovitch, M. C. (2021, August). Elephants evolved strategies reducing the biomechanical complexity of their trunk. *Current Biology*. doi: 10.1016/j.cub.2021.08.029

Emmons, L. H., & Gentry, A. H. (1983, April). Tropical Forest Structure and the Distribution of Gliding and Prehensile-Tailed Vertebrates. *The American Naturalist*, *121*(4), 513–524. Retrieved 2022-09-14, from `https://www.journals.uchicago.edu/doi/abs/10.1086/284079` (Publisher: The University of Chicago Press) doi: 10.1086/284079

Gao, X., Wang, L., & Hao, X. (2015, August). An improved Capstan equation including power-law friction and bending rigidity for high performance yarn. *Mechanism and Machine Theory*, *90*, 84–94. Retrieved 2021-05-03, from `https://www.sciencedirect.com/science/article/pii/S0094114X15000427` doi: 10.1016/j.mechmachtheory.2015.03.005

Garber, P., & Rehg, J. (1999). The ecological role of the prehensile tail in white-faced capuchins (Cebus capucinus). *American Journal of Physical Anthropology*, *110*(3), 325–339. (_eprint: https://onlinelibrary.wiley.com/doi/pdf/10.1002/%28SICI%291096-8644%28199911%29110%3A3%3C325%3A%3AAID-AJPA5%3E3.0.CO%3B2-D) doi: 10.1002/(SICI)1096-8644(199911)110:3⟨325::AID-AJPA5⟩3.0.CO;2-D

Hickman, G. C. (1979). The mammalian tail: a review of functions. *Mammal Review*, *9*(4), 143–157. (_eprint: https://onlinelibrary.wiley.com/doi/pdf/10.1111/j.1365-2907.1979.tb00252.x) doi: 10.1111/j.1365-2907.1979.tb00252.x

Hoffmann, J. N., Montag, A. G., & Dominy, N. J. (2004). Meissner corpuscles and somatosensory acuity: The prehensile appendages of primates and elephants. *The Anatomical Record Part A: Discoveries in Molecular, Cellular, and Evolutionary Biology*, *281A*(1), 1138–1147. (_eprint: https://onlinelibrary.wiley.com/doi/pdf/10.1002/ar.a.20119) doi: 10.1002/ar.a.20119

Iberall, T. (1997, June). Human Prehension and Dexterous Robot Hands. *The International Journal of Robotics Research*, *16*(3), 285–299. (Publisher: SAGE Publications Ltd STM) doi: 10.1177/027836499701600302

Jones, R. M., Fry, A. C., Weiss, L. W., Kinzey, S. J., & Moore, C. A. (2008, November). Kinetic Comparison of Free Weight and Machine Power Cleans:. *Journal of Strength and Conditioning Research*, *22*(6), 1785–1789. Retrieved 2018-09-20, from https://insights.ovid.com/crossref?an=00124278-200811000-00010 doi: 10.1519/JSC.0b013e318185f068

Jones-Engel, L. E., & Bard, K. A. (1996). Precision grips in young chimpanzees. *American Journal of Primatology*, *39*(1), 1–15. (_eprint: https://onlinelibrary.wiley.com/doi/pdf/10.1002/%28SICI%291098-2345%281996%2939%3A1%3C1%3A%3AAID-AJP1%3E3.0.CO%3B2-2) doi: 10.1002/(SICI)1098-2345(1996)39:1⟨1::AID-AJP1⟩3.0.CO;2-2

Laska, M. (1996, December). Manual Laterality in Spider Monkeys (Ateles geoffroyi) Solving Visually and Tactually Guided Food-Reaching Tasks. *Cortex*, *32*(4), 717–726. Retrieved 2022-09-14, from https://www.sciencedirect.com/science/article/pii/S0010945296800414 doi: 10.1016/S0010-9452(96)80041-4

Laska, M. (1998, January). Laterality in The Use of The Prehensile Tail in The Spider Monkey (Ateles geoffroyi). *Cortex*, *34*(1), 123–130. Retrieved 2022-09-14, from https://www.sciencedirect.com/science/article/pii/S001094520870741X doi: 10.1016/S0010-9452(08)70741-X

Lourie, S. A., Pollom, R. A., & Foster, S. J. (2016, August). A global revision of the Seahorses Hippocampus Rafinesque 1810 (Actinopterygii: Syngnathiformes): Taxonomy and biogeography with recommendations for further research. *Zootaxa*, *4146*(1), 1–66. Retrieved 2022-09-14, from https://www.mapress.com/zt/article/view/zootaxa.4146.1.1 (Number: 1) doi: 10.11646/zootaxa.4146.1.1

Marvi, H., Meyers, G., Russell, G., & Hu, D. L. (2011, January). Scalybot: A Snake-Inspired Robot With Active Control of Friction. In *ASME 2011 Dynamic Systems and Control Conference and Bath/ASME Symposium on Fluid Power and Motion Control, Volume 2* (pp. 443–450). Arlington, Virginia, USA: ASMEDC. Retrieved 2021-07-06, from https://asmedigitalcollection.asme.org/DSCC/proceedings/DSCC2011/54761/443/353640 doi: 10.1115/DSCC2011-6174

McGinn, C. (2015). *Prehension: The Hand and the Emergence of Humanity*. MIT Press. (Google-Books-ID: MGV0CgAAQBAJ)

Negrea, S., Botnariuc, N., & Dumont, H. J. (1999, October). Phylogeny, evolution and classification of the Branchiopoda (Crustacea). *Hydrobiologia*, *412*(0), 191–212. Retrieved 2022-09-14, from https://doi.org/10.1023/A:1003894207100 doi: 10.1023/A:1003894207100

Organ, J. M., Muchlinski, M. N., & Deane, A. S. (2011). Mechanoreceptivity of Prehensile Tail Skin Varies Between Ateline and Cebine Primates. *The Anatomical Record*, *294*(12), 2064–2072. (_eprint: https://onlinelibrary.wiley.com/doi/pdf/10.1002/ar.21505) doi: 10.1002/ar.21505

Porter, M. M., Adriaens, D., Hatton, R. L., Meyers, M. A., & McKittrick, J. (2015, July). Why the seahorse tail is square. *Science*, *349*(6243), aaa6683. Retrieved 2022-09-14, from https://www.science.org/doi/full/10.1126/science.aaa6683 (Publisher: American Association for the Advancement of Science) doi: 10.1126/science.aaa6683

Pretorius, Y., de Boer, W. F., Kortekaas, K., van Wijngaarden, M., Grant, R. C., Kohi, E. M., ... Prins, H. H. T. (2016, April). Why elephant have trunks and giraffe long tongues: how plants shape large herbivore mouth morphology. *Acta Zoologica*, *97*(2), 246–254. Retrieved 2018-09-19, from http://doi.wiley.com/10.1111/azo.12121 doi: 10.1111/azo.12121

Read, W. T. (1937, January). Handbook of Engineering Fundamentals (Eshbach, Ovid W., ed.). *Journal of Chemical Education*, *14*(1), 49. Retrieved from https://doi.org/10.1021/ed014p49.2 doi: 10.1021/ed014p49.2

Russo, G. A., & Young, J. W. (2011). Tail growth tracks the ontogeny of prehensile tail use in capuchin monkeys (Cebus albifrons and C. apella). *American Journal of Physical Anthropology*, *146*(3), 465–473. (_eprint: https://onlinelibrary.wiley.com/doi/pdf/10.1002/ajpa.21617) doi: 10.1002/ajpa.21617

Schulz, A. K., Boyle, M., Boyle, C., Sordilla, S., Rincon, C., Hooper, S., … Hu, D. L. (2022, August). Skin wrinkles and folds enable asymmetric stretch in the elephant trunk. *Proceedings of the National Academy of Sciences*, *119*(31), e2122563119. Retrieved 2022-09-12, from `https://www.pnas.org/doi/abs/10.1073/pnas.2122563119` (Publisher: Proceedings of the National Academy of Sciences) doi: 10.1073/pnas.2122563119

Schulz, A. K., Ning Wu, J., Ha, S. Y. S., Kim, G., Braccini Slade, S., Rivera, S., … Hu, D. L. (2021). Suction feeding by elephants. *Journal of The Royal Society Interface*, *18*(179), 20210215. Retrieved 2021-06-16, from `https://royalsocietypublishing.org/doi/10.1098/rsif.2021.0215` (Publisher: Royal Society) doi: 10.1098/rsif.2021.0215

Wilson, J. F., Mahajan, U., Wainwright, S. A., & Croner, L. J. (1991). A Continuum Model of Elephant Trunks. *Journal of Biomechanical Engineering*, *113*(1), 79. Retrieved 2018-07-20, from `http://Biomechanical.asmedigitalcollection.asme.org/article.aspx?articleid=1398531` doi: 10.1115/1.2894088

Wright, P., & Luck, C. (1984, January). Do elephants need to sweat? *South African Journal of Zoology*, *19*(4), 270–274. (Publisher: Taylor & Francis _eprint: https://doi.org/10.1080/02541858.1984.11447892) doi: 10.1080/02541858.1984.11447892

Wu, J., Zhao, Y., Zhang, Y., Shumate, D., Slade, S. B., Franklin, S. V., & Hu, D. L. (2018). Elephant trunks form joints to squeeze together small objects. *Journal of The Royal Society Interface*, 9.

Yum, S.-M., Baek, I.-K., Hong, D., Kim, J., Jung, K., Kim, S., … Park, G.-S. (2020, December). Fingerprint ridges allow primates to regulate grip. *Proceedings of the National Academy of Sciences*, *117*(50), 31665–31673. Retrieved 2022-04-24, from `https://www.pnas.org/doi/10.1073/pnas.2001055117` (Publisher: Proceedings of the National Academy of Sciences) doi: 10.1073/pnas.2001055117

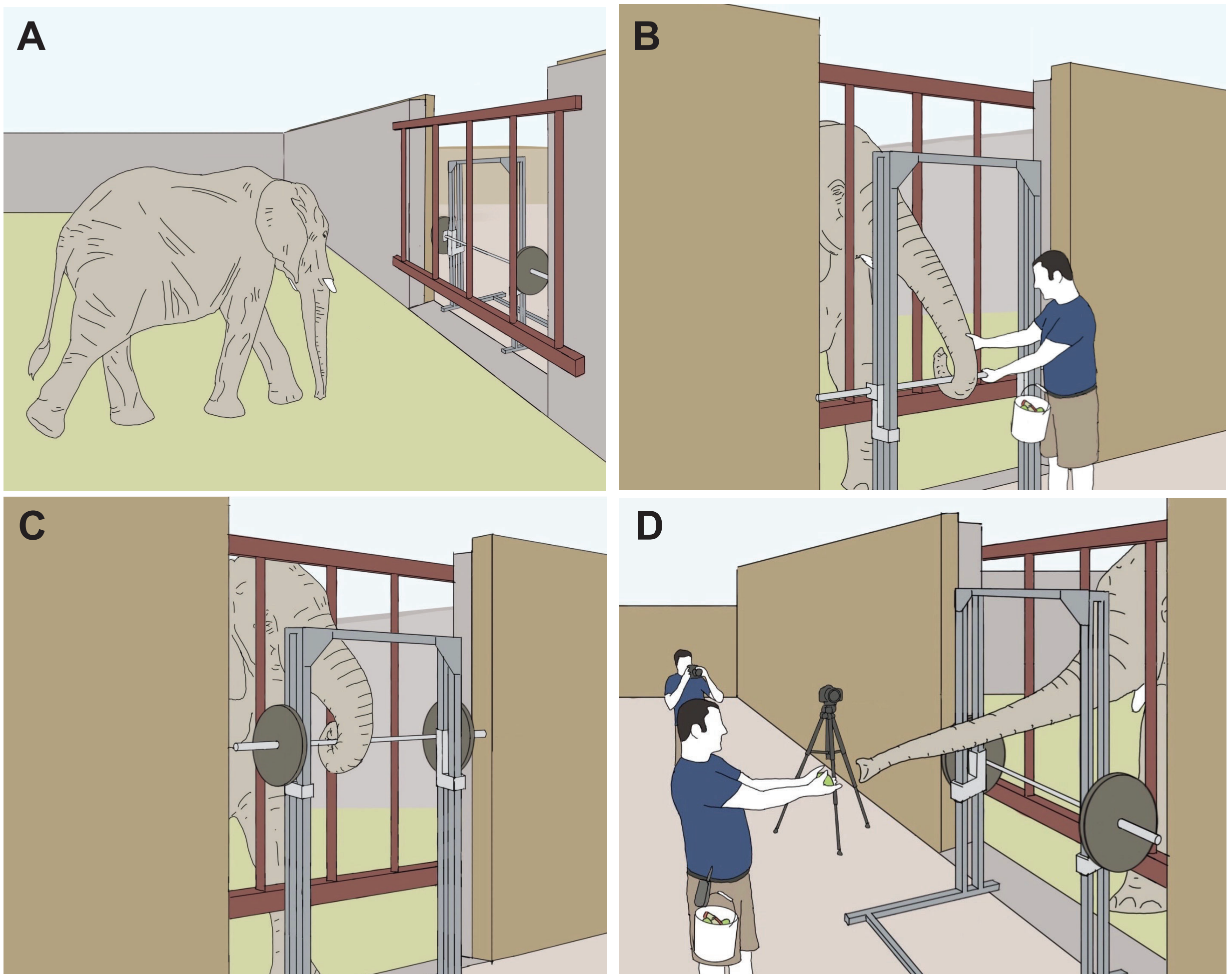

Figure 1: Illustration sequence showing the procedures for elephant lifting the barbell. a) The African elephant *Loxodonta africana* approaches the barbell setup for experimental procedure. b) Zoo Atlanta elephant keepers showing elephant how to wrap around the barbell and lift it. c) Elephant completing a trial with a heavier weight. d) After completing a trial, the elephant reaches out to Zoo Atlanta keeper for food incentive. Illustrations by Benjamin Seleb.

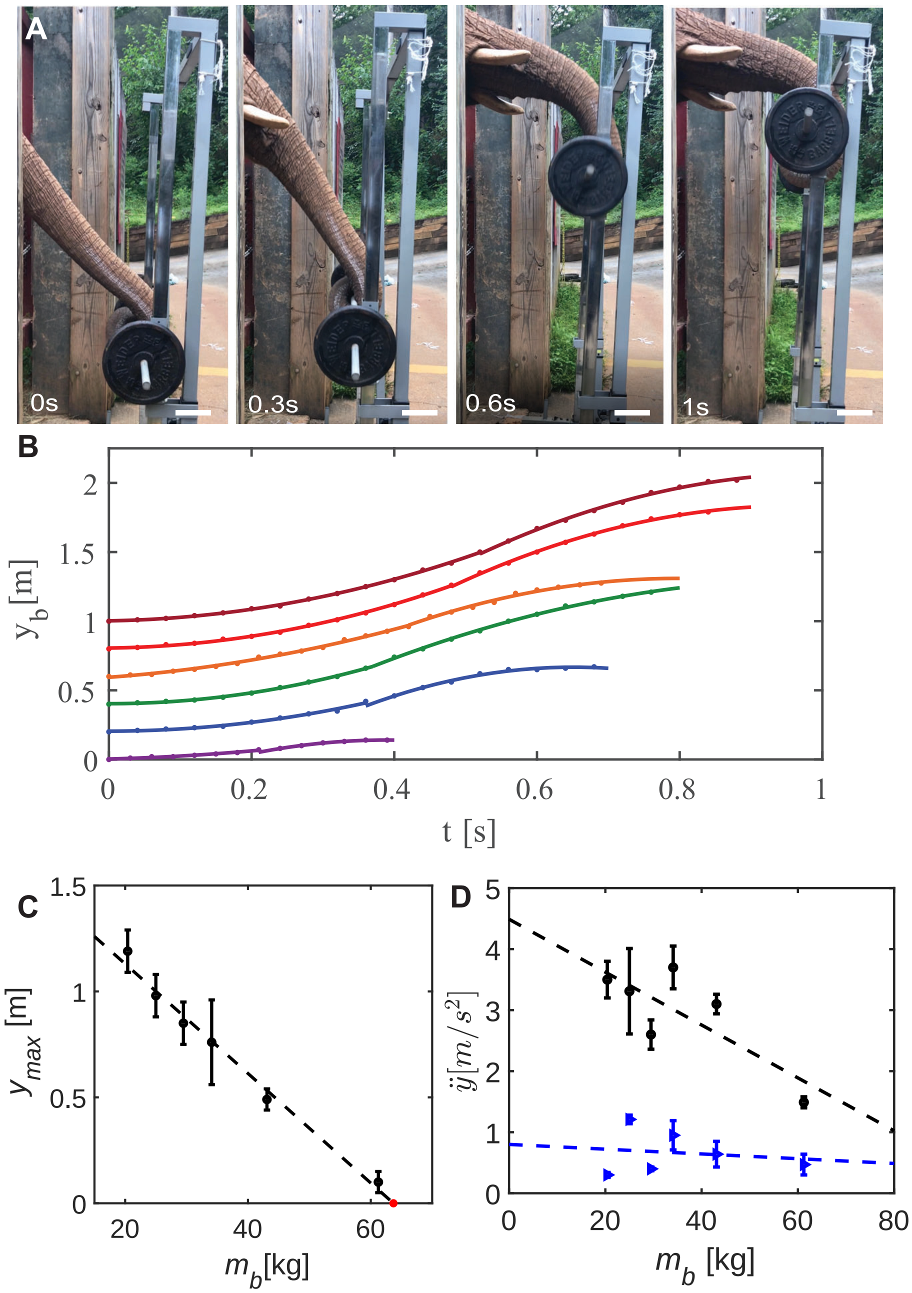

Figure 2: Kinematics of weight lifting. a) Time series of the elephant lifting a barbell at increments of 0.3s with scale bars showing 10 cm. b) Time course of the position of the barbell, with increments given between trajectory given for clarity. Weights include: maaroon (20kg), red (25 kg), orange (30 kg), green (34 kg), blue (43 kg), purple (60 kg). Solid lines are best fit lines associated with constant acceleration a and constant deceleration. c) Relationship between maximum height of the elephant trunk and the barbell mass with red dot indicating the x-intercept, which is the maximum mass that the can be lifted in this setup. d) Relationship between vertical acceleration and barbell mass. The barbell and the base of the trunk are shown by black circles and blue triangles, respectively. Best fits given by the dashed lines.

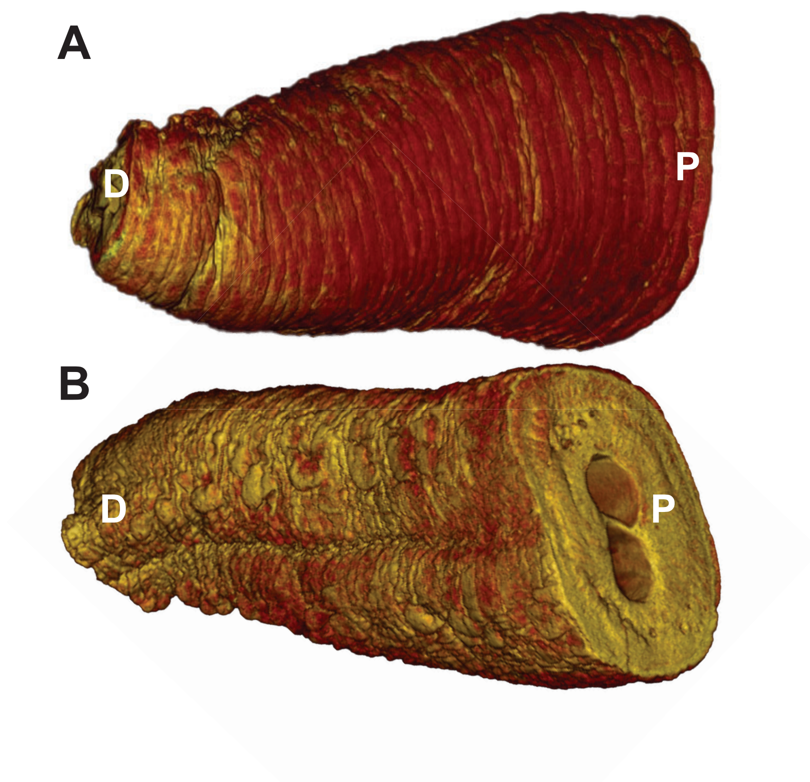

Figure 3: CT scan of the distal 60-cm of the trunk of a 38 year old female African elephant *Loxodonta africana*. a) dorsal section and b) ventral section. P refers to proximal (towards the skull), D refers to distal (towards the tip) at a distance of 60 cm from the tip.

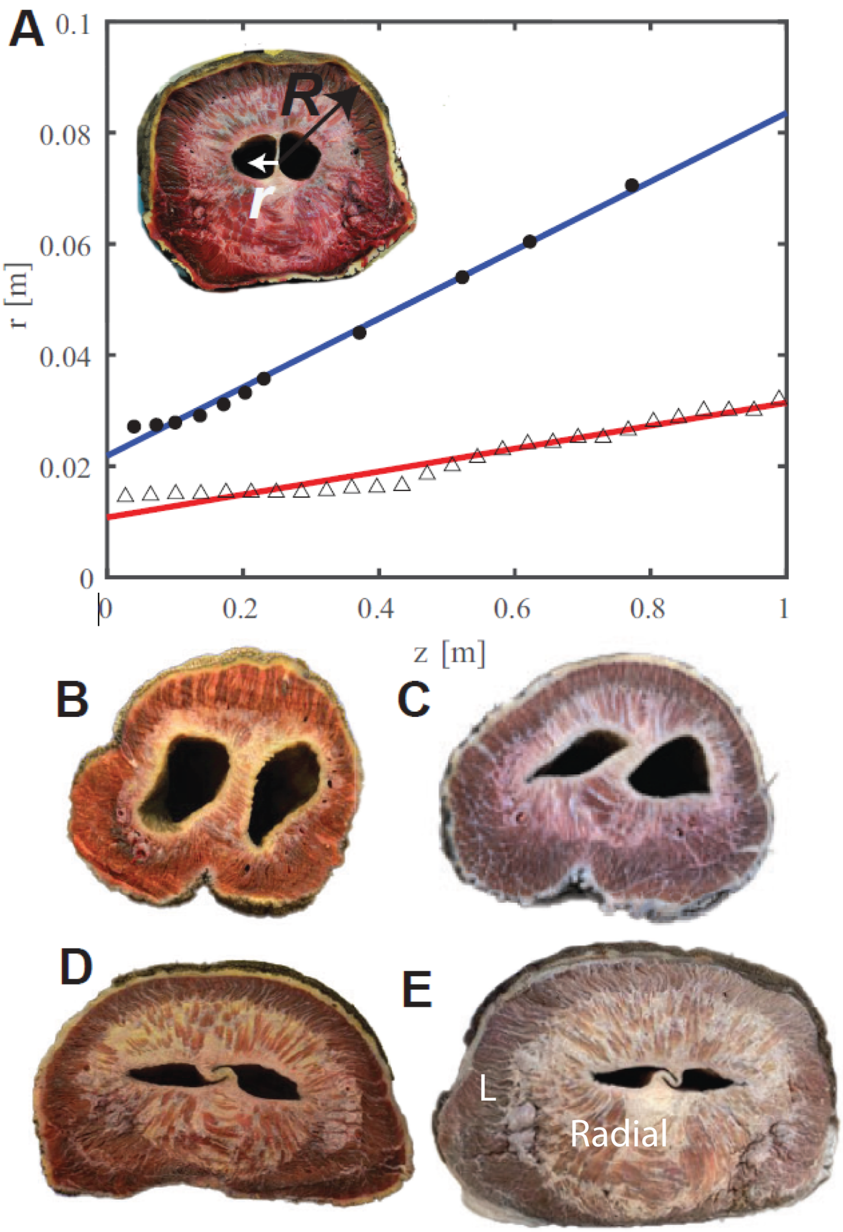

Figure 4: Elephant trunk anatomy. a) The relationship between radius of trunk and distance z from the tip. The trunk outer radius, R is given by the shaded circles and inner nasal radius, r by open triangles. Linear best fits are shown by the solid lines. b-e) Elephant trunk cross sections displaying muscle fibers and negative space created by nasal passageway. b) cross section 28 cm from distal tip. c) 56 cm from distal tip. d) 100 cm from distal tip. e) 140 cm from distal tip With L indicating longitudinal muscles, and radial muscles labeled on the cross section.

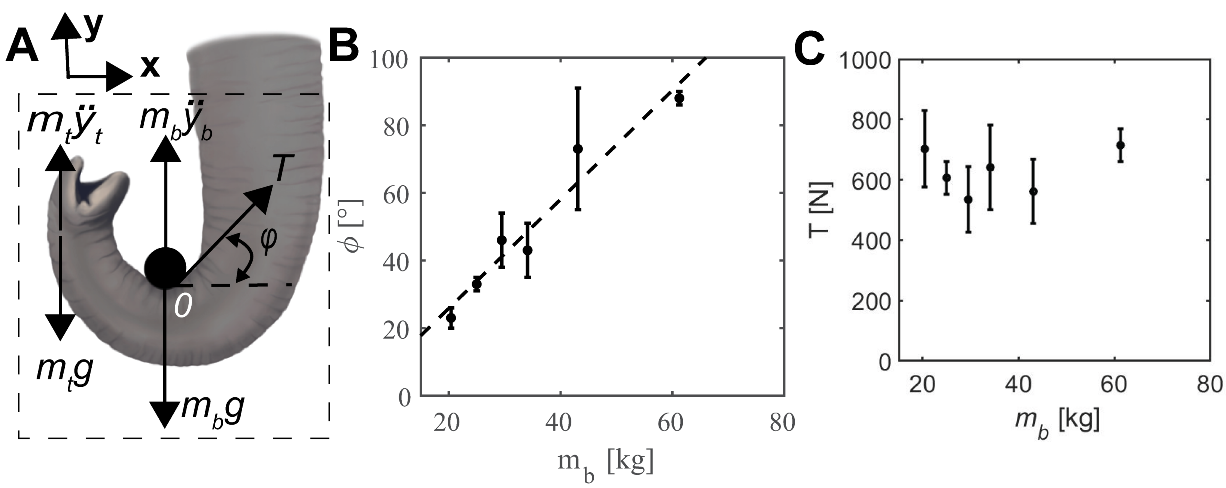

Figure 5: Forces exerted on the barbell. a) Free body diagram of elephant lifting a barbell. The elephant applies a tension T to the barbell to lift it at contact point O. The trunk is at an angle of contact ϕ with respect to the horizontal. The combined trunk and barbell mass experiences gravity g and an upward acceleration $\ddot{y}$. b) The relationship between angle of contact ϕ and barbell mass with linear best fit given by the dashed line. c) The relationship between tension T and barbell mass.

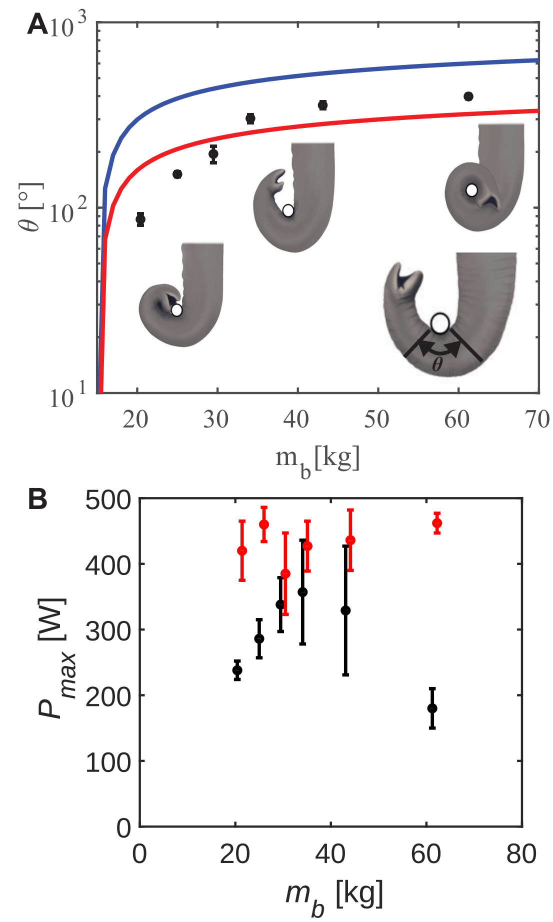

Figure 6: Elephants wrap the trunk to lift heavier weights. a) The relationship between angle of trunk wrap θ and barbell mass. Schematics, from left to right, show the increasing wrapping of the trunk for barbell weights 20 kg, 25 kg, and 60 kg. Theoretical predictions with friction coefficient of 0.5 and 1.5 are shown by the blue and red lines, respectively. b) Maximum power exerted to lift different barbell masses. Power is calculated at two locations, the distal tip (black circles) and the proximal root (red circles).

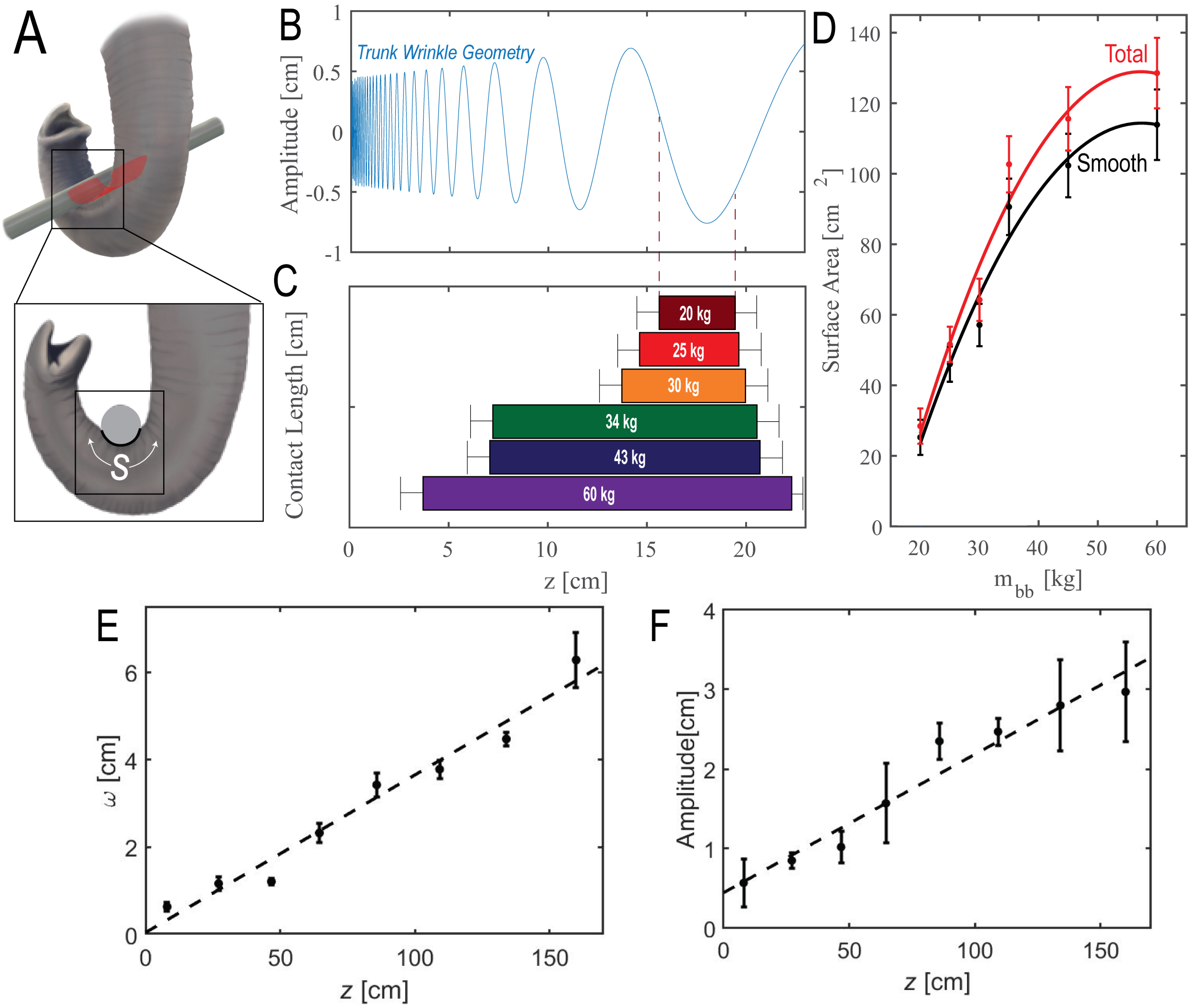

Figure 7: Elephants adjust grip to allow more wrinkled contact with the barbell. a) Schematic displaying the elephant's area of contact with the barbell. Last insent shows magnfication indicating that the wrinkles increase the surface area. b) Surface profile along the trunk's longitudinal direction. Wrinkles increase in amplitude and wavelength with distnace from the tip, which is at z=0. c) Total contact length s of the barbell for different barbell weights. d) Surface area of contact across weight classes, with black showing the surface area without wrinkles and red the surface area with wrinkles included. e) Wavelength of the elephant wrinkles from the tip of the trunk to the base. f) Amplitude of the elephant wrinkles from the tip of the trunk to the base.